Large-area ultrathin films of reduced graphene oxide as a transparent and flexible electronic material

GOKI EDA, GIOVANNI FANCHINI AND MANISH CHHOWALLA*

Materials Science and Engineering, Rutgers University, 607 Taylor Road, Piscataway, New Jersey 08854, USA
***e-mail: manish1@rci.rutgers.edu**

Published online: 6 April 2008; doi:10.1038/nnano.2008.83

The integration of novel materials such as single-walled carbon nanotubes and nanowires into devices has been challenging, but developments in transfer printing and solution-based methods now allow these materials to be incorporated into large-area electronics[1–6]. Similar efforts are now being devoted to making the integration of graphene into devices technologically feasible[7–10]. Here, we report a solution-based method that allows uniform and controllable deposition of reduced graphene oxide thin films with thicknesses ranging from a single monolayer to several layers over large areas. The opto-electronic properties can thus be tuned over several orders of magnitude, making them potentially useful for flexible and transparent semiconductors or semi-metals. The thinnest films exhibit graphene-like ambipolar transistor characteristics, whereas thicker films behave as graphite-like semi-metals. Collectively, our deposition method could represent a route for translating the interesting fundamental properties of graphene into technologically viable devices.

Electronic devices constructed from a single layer of graphite, referred to as graphene[11], have received significant attention. Graphene is a 0 eV bandgap semiconductor in which the filled valence band touches the empty conduction band, thus giving rise to peculiar properties[12] that could have particularly interesting applications in electronic devices[13–16]. The discovery of isolated graphene obtained from the simple mechanical cleaving 'Scotch tape method'[11] has made fabrication of devices on individual graphene sheets straightforward. Effort is also under way to grow large-area epitaxial graphene[17,18]. In addition, promising approaches based on transfer printing of exfoliated graphene onto electrodes on different substrates for large-scale integration have been reported recently[7–9].

In addition to individual sheet devices, efforts to obtain graphene-based composites through the reduction of graphene oxide (GO) in solution and incorporation into hosts have also yielded promising results[19]. Recently, there have been reports of non-composite reduction of GO into graphene using chemical routes and high-temperature annealing[20–25]. The chemical approach is appealing because it opens a route for the deposition of graphene from solution, allowing devices to be fabricated on virtually any surface.

We describe a simple and reproducible method to uniformly deposit between one and five layers of graphene from reduced GO in the form of thin films to create transistors and proof-of-concept electrodes for organic photovoltaics (see Supplementary Information). A GO aqueous suspension can be readily obtained from exfoliation of graphite through oxidation[26,27] (see Methods). Methods such as drop casting[20,24], rapid freezing by spraying[21] and dip coating[22] from GO suspension have been used to obtain isolated individual and multilayered sheets or thin films. In order to reproducibly achieve uniform thin films with a controllable number of GO layers over large areas, we have used the vacuum filtration method, which has been used widely to deposit highly uniform single-walled carbon nanotube (SWNT) thin films[2,28,29].

Vacuum filtration involves the filtration of a GO suspension through a commercial mixed cellulose ester membrane with an average pore size of 25 nm. As the suspension is filtered through the ester membrane, the liquid is able to pass through the pores, but the GO sheets become lodged. The permeation rate of the solvent is controlled by the accumulation of the GO sheets on the pores so as the number of GO layers increases at a given location on the porous membrane, the rate of filtration decreases, but does so to a lesser degree at thinner or uncovered regions. The process is therefore self-regulating, which allows reasonably good nanoscale control over the film thickness by simply varying either the concentration of the GO in the suspension or the filtration volume. The GO flakes on the filter membrane can then be transferred by placing the membrane with the film side down onto a substrate and dissolving the membrane with acetone, leaving behind a uniform GO thin film (see Methods for details). The yield of the transfer process is nearly 100%, independent of the substrate, indicating that van der Waals interactions give rise to sufficiently strong cohesive forces within the film and also between the GO sheets and the substrate to obtain a well adhered uniform film. Indeed, the as-deposited thin films of GO are able to withstand typical lithographic processes (rinsing, blowing with dry nitrogen and deposition of electrodes) without any evidence of delamination. A GO thin film covering an area of 10 cm^2 on an ester membrane is shown in Fig. 1a, and transferred films on glass and plastic substrates are shown in Fig. 1b,c, respectively.

The thicknesses obtained by atomic force microscope (AFM) profilometry, ellipsometry and Raman spectroscopy were found to be 1–2 nm for the films deposited at a filtration volume of 20 ml and 3–5 nm at 80 ml, suggesting that the thinnest films consist of single layers of GO (ref. 23) (concentration = 0.33 mg l^{-1}; see Supplementary Information for experimental

Figure 1 Thin films of solution-processed GO. a–c, Photographs of GO thin films on filtration membrane (**a**), glass (**b**) and plastic (**c**) substrates.

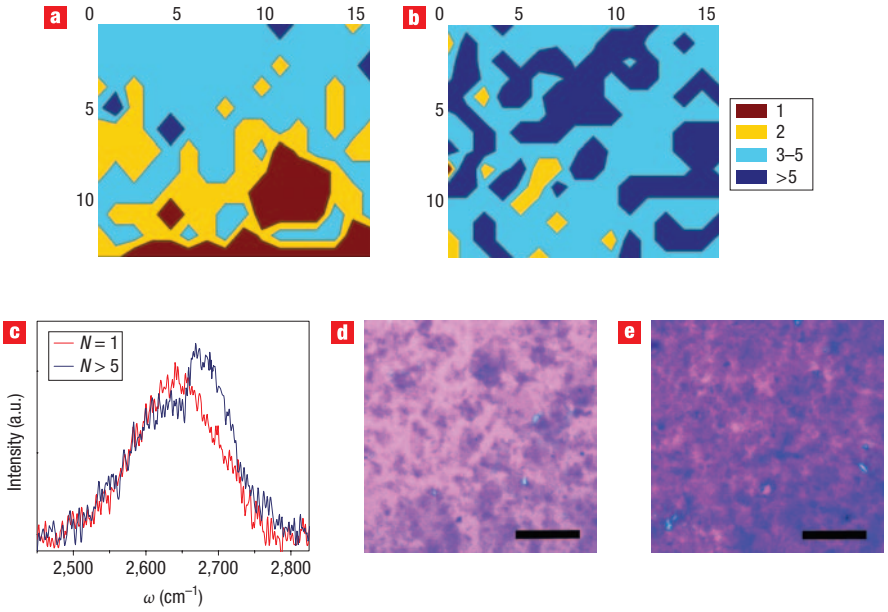

Figure 2 Characterization of reduced GO thin films using Raman spectroscopy. a,**b**, Raman maps (15 μm × 12 μm) for 20 ml (**a**) and 80 ml (**b**) reduced GO thin films, in which the different colours indicate different numbers of graphene layers, as shown in the key. **c**, Raman spectra near the 2D peak for a single-layer region ($N = 1$) and for a multiple-layer region ($N > 5$). **d**,**e**, Optical micrographs of 20 ml (**d**) and 80 ml (**e**) films showing the different densities of the overlapped regions (darker colours) between the graphene sheets (scale bar = 20 μm).

details and AFM images). It should be noted that pure single-layer graphene flake has a thickness of 0.34 nm, corresponding to the interlayer spacing of graphite, but a GO sheet is ~1 nm thick due to the presence of functional groups, structural defects and adsorbed water molecules[25,30].

We also investigated the number of reduced GO layers using Raman spectroscopy by monitoring the second-order zone boundary phonons peak at 2,700 cm^{-1}, referred to as the G′ or 2D peak[31] (see Methods). Raman spectra of reduced GO thin films typically show the presence of the usual D, G and 2D peaks[31] (see Supplementary Information). The prominent D peak (absent in mechanically cleaved graphene) clearly indicates the presence of structural imperfections induced by the attachment of hyrodxyl and epoxide groups on the carbon basal plane. The intensity of the 2D peak with respect to the D and G peaks is small due to disorder, and thus requires care during acquisition and analysis. Nevertheless, the shift in this peak can be used as a simple non-destructive tool for analysing the number of layers in graphene[31]. Careful analysis of the spectra allowed us to monitor the 2D peak shifts and thus map the number of reduced GO layers in the thin films. The Raman maps over 15 μm × 12 μm spatial regions for the 20 ml and 80 ml reduced GO thin films are shown in Fig. 2a and b. The 2D peak shift between one and more than five layers of graphene was found to be approximately 40 cm^{-1} wavenumbers, as indicated by the actual measured peaks shown in Fig. 2c.

The Raman maps are consistent with the AFM data in that the percolating regions consist of 1–2 and 3–5 layers in both the 20 and 80 ml thin films. However, it can be seen from Fig. 2a that 1–2 layers are more predominant in the 20 ml film compared to the 80 ml film, where 3–5 layers are more readily visible. In addition, thicker regions (>5 layers) are also visible in the Raman maps, which likely arise from incomplete exfoliation of GO in suspension[24]. The optical images of the 20 ml and 80 ml films are shown in Fig. 2d and e to indicate the degree of overlapping (darker regions) among the GO layers. The darker

regions are clearly less visible in the 20 ml film. Our thickness results suggest that the thin films are uniform in that they contain 1–5 layers of reduced GO. However, the slight variation in thicknesses in Raman maps of both films point to the fact that a better control of the size and shape of the suspended GO sheets will be essential if films of exactly a single monolayer are to be deposited.

After deposition, the insulating GO must be reduced to graphene through exposure to hydrazine vapour and/or annealing in inert conditions[19–21,23–25,30,32] to render the material electrically conductive. We found that the hydrazine vapour alone is not sufficient to achieve maximum reduction, and annealing alone requires relatively high temperatures (>550 °C)[22]. Efficient reduction of the GO thin films was therefore achieved through a combination of hydrazine vapour exposure and low-temperature annealing treatment (see Supplementary Information for X-ray photoelectron spectroscopy (XPS) results)[30,32]. The reduction of GO yields thin films with properties resembling those of graphene. More interestingly, by controlling the amount of reduced GO on the surface, it is possible to tune the optoelectronic properties of the thin films as summarized in Fig. 3a,b. It can be seen from Fig. 3a that the sheet resistance of the hydrazine-treated GO thin films is independent of the filtration volume except at very high values (>300 ml). However, annealing at 200 °C in nitrogen (or vacuum) leads to a dramatic reduction in the sheet resistance ($\sim 1 \times 10^5\ \Omega\,\square^{-1}$). The lowest sheet resistance value we obtained was $\sim 43\ \mathrm{k}\Omega\,\square^{-1}$. The saturation of sheet resistance in Fig. 3a above a critical filtration volume is probably due to the fact that reduction is only effective for the uppermost layers. The corresponding transmittances as a function of the filtration volume at $\lambda = 550$ nm for the as-deposited GO, chemically reduced GO and chemically reduced and annealed GO are shown in Fig. 3b (see Supplementary Information for transmission versus wavelength plots). It can be seen that the chemically reduced and annealed GO leads to a decrease in the transparency of thin films that is lower than that for reduced and non-annealed GO, also consistent with the increase in the Drude background obtained from spectroscopic ellipsometry (see Supplementary Information).

In order to translate the opto-electronic properties into devices, we fabricated thin-film transistors (TFTs) with reduced GO thin films. Of the numerous (>100) TFT devices we tested, all showed uniform transfer characteristics regardless of the channel length (21 μm or 210 μm, SiO_2 thickness = 300 nm, channel width = 400 μm). The relatively long channel lengths ensured that the transport was bulk limited and the role of contacts was not substantial in our devices. The transfer characteristics as a function of temperature for the 20 and 80 ml reduced GO thin films are shown in Fig. 4a,b, respectively, together with a photograph of the devices (Fig. 4c). The low-temperature measurements exhibit ambipolar characteristics, comparable to graphene. This is remarkable, because transport between the source and drain electrodes in our large-scale devices occurs over several graphene sheets. The p-type oxygen doping effect[11], which increases the current and shifts the threshold voltage to positive voltages, is dramatically reduced for both the 20 ml and 80 ml devices when measurements are performed in vacuum. The primary differences between the two devices are that the current in the 80 ml TFTs is higher and the 20 ml device exhibits a sharper turn on behaviour, which is consistent with conduction occurring primarily through one or two layers of graphene. In addition, the 'V' shape of the ambipolar graphene transfer characteristics is more pronounced for the low-temperature measurements of the 20 ml TFTs, suggesting the semiconducting nature of the material. The mobility of the devices in ambient conditions calculated from the linear regime of the transfer

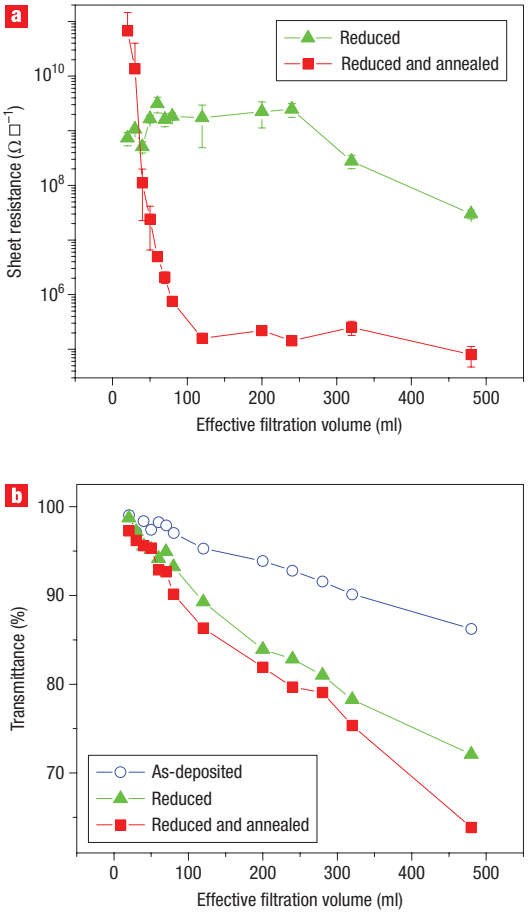

Figure 3 Electrical and optical properties of reduced GO thin films. a,b, Sheet resistance (**a**) and transmittance (**b**) at $\lambda = 550$ nm as a function of filtration volume for reduced GO thin films. Plots are shown for thin films with different reduction steps. The sheet resistance for as-deposited GO thin films is out of scale.

characteristics (see Methods and Supplementary Information) was found to be $\sim 1\ \mathrm{cm}^2\,\mathrm{V}^{-1}\,\mathrm{s}^{-1}$ for holes and was lower at low temperatures. The electron mobilities ($\sim 0.2\ \mathrm{cm}^2\,\mathrm{V}^{-1}\,\mathrm{s}^{-1}$) were generally lower than the hole mobilities at ambient conditions, and the reverse was true in vacuum. The lower overall mobilities in our devices compared to those achieved in individual reduced GO flakes ($2–200\ \mathrm{cm}^2\,\mathrm{V}^{-1}\,\mathrm{s}^{-1}$) could be attributed to scattering at the junctions formed by overlapping flakes. The electron and hole currents from TFTs and conductivity versus temperature for the 20 ml thin films are shown in Fig. 4d,e, respectively. The temperature dependence is unusual but consistent with the anomalous behaviour found in exfoliated graphite[33], in which conduction is metallic-like below ~50 K and then crosses over to activated transport above this temperature.

A method is reported for uniform and controllable deposition of 1–5 nm graphene thin films from solution at room temperature on a variety of substrates, from the reduction of GO. The vacuum filtration method allows the deposition of very thin films of 1–2 layers of reduced GO that are semiconducting, and thicker films that are semi-metallic. We have demonstrated that the sheet resistance of the thin films can be tuned over six orders of magnitude and the transparencies from 60 to 95%. The deposition of uniform thin films allows the simple fabrication of TFTs on various substrates without the use of extensive lithography. Our

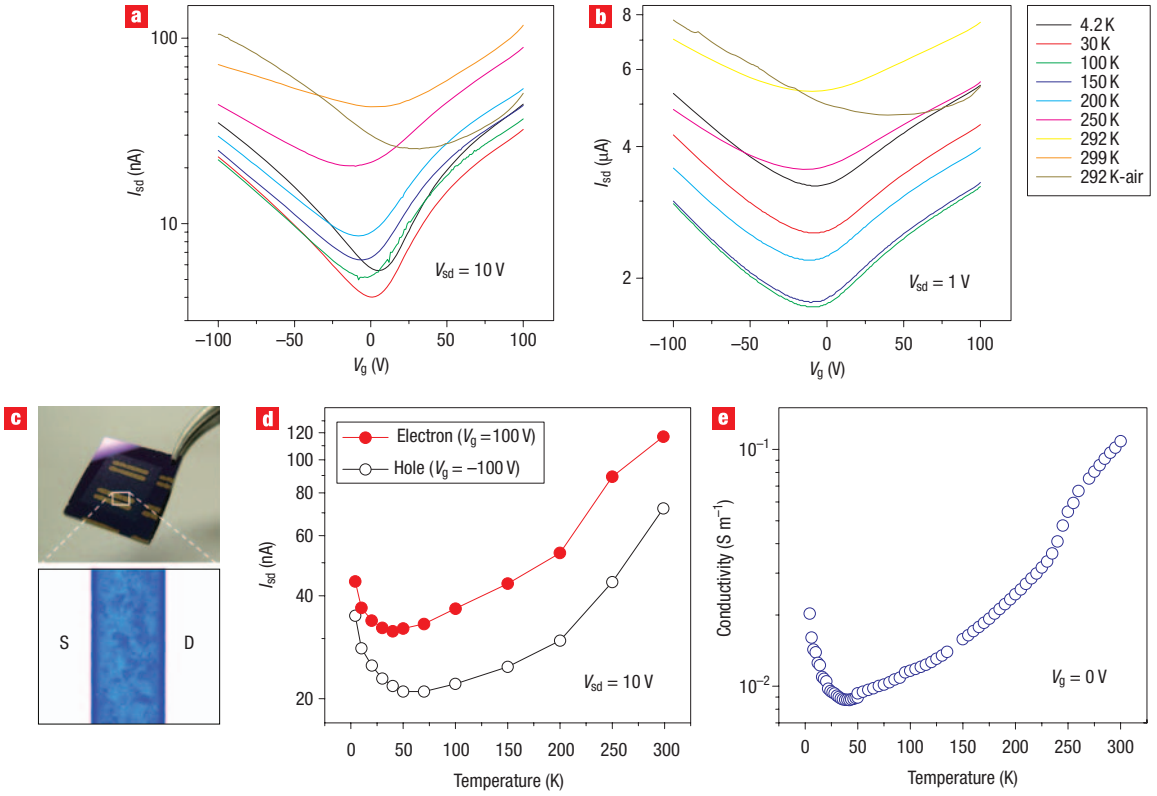

Figure 4 TFT devices based on reduced GO thin films. a,**b**, Source–drain current as a function of gate voltage for 20 ml (**a**) and 80 ml (**b**) films measured at different temperatures. Measurements were conducted in vacuum unless otherwise noted. **c**, An optical micrograph of the actual device. The channel consists of several reduced GO sheets percolating across the source (S) and drain (D) electrodes. The channel length is 21 μm. **d**, Electron and hole currents at maximum and minimum gate voltages as a function of temperature for the 20 ml film. **e**, Film conductivity as a function of temperature (film thickness of 2 nm is assumed) exhibiting anomalous behaviour.

results could provide a pathway for the translation of graphene-based research from the fundamental to the technological realm.

METHODS

Slurry of GO was obtained from SP-1 graphite (Bay Carbon) using the modified Hummers method[27]. The concentration of the slurry was determined by drying GO over phosphorus pentoxide in a vacuum desiccator for a week and was found to be 49 mg ml^{-1}. The slurry was diluted in water and sonicated to achieve exfoliated sheets of GO. The effective filtration volume mentioned in the manuscript indicates volumes of 0.33 mg l^{-1} suspension required to achieve the mass deposited by suspension of other concentrations. For example, films obtained by filtrating 60 ml of 0.66 mg l^{-1} suspension are indicated as a 120 ml film. A dilute GO suspension (0.33–2.64 mg l^{-1}) was vacuum-filtrated using a mixed cellulose ester membrane with 25 nm pores (Millipore). The membranes with captured GO were then cut into sizes of choice, wetted with deionized water, and pressed against the substrate surface with the GO side in contact with the substrate. The GO film was allowed to dry and adhere to the substrate at room temperature under a 1 kg weight for at least 10 h. The weight was removed and the membrane was dissolved using acetone (successively pure baths) to leave a GO thin film on the substrate. The films were then rinsed with a methanol wash and dried by blowing with dry nitrogen. Similar to the SWNT thin films, the adhesion of the GO thin films was found to be sufficiently strong to prevent delamination during processing.

Unpolarized Raman spectra were recorded at room temperature on reduced GO thin films deposited on 300-nm-thick SiO_2. A Renishaw InVia Raman microscope equipped with a ×100 objective was used. The excitation source was the 633 nm line from a He–Ne laser and the spot size was estimated to be less than 2 μm. Low power and special attention was used to avoid laser heating of the specimen. Sample areas up to 15 × 12 μm were mapped using a precision *xyz* stage and the Renishaw 2.0 mapping software. According to recent studies[31], the peak position of the second-order Raman D-peak, f(2D), considerably blueshifts with increasing number of layers in graphene. Therefore, we were able to reconstruct the number of layers in our samples by mapping f(2D) in our films. The 2D peak positions we assumed for one, two and a few layers of graphene in order to reconstruct the maps were taken from other work[31] (see Supplementary Information, Table S1). Such values of f(2D) allowed us to obtain the maps reported in Fig. 2a and b, which were reconstructed from the raw data using the Matlab 6.5 Contour routine. Comparison of spectra recorded from thick (>5 layers) and thin (1 layer) regions of the 80 ml films are reported in Fig. 2c. In addition to the 20 and 80 ml samples, we also measured the number of layers for a 50 ml sample (see Supplementary Information).

Bottom-gated TFTs were fabricated by depositing and reducing GO on p-Si substrates with 300 nm thermal oxide. p-Si was used as the gate electrode. We arbitrarily deposited gold source and drain electrodes with channel lengths of 21 μm and 210 μm to investigate the uniformity of the thin films. The mobility was calculated using $\mu = (L/WC_{ox}V_{sd})(\Delta I_{sd}/\Delta V_g)$, where L and W are the channel length and width, C_{ox} the gate oxide capacitance, V_{sd} the source–drain voltage, I_{sd} the source–drain current and V_g the gate voltage. The linear regime of the transfer characteristics was used to obtain $\Delta I_{sd}/\Delta V_g$ (see Supplementary Information for details).

Received 4 February 2008; accepted 5 March 2008; published 6 April 2008.

References

1. Ahn, J. H. *et al.* Heterogeneous three-dimensional electronics by use of printed semiconductor nanomaterials. *Science* **314,** 1754–1757 (2006).
2. Wu, Z. C. *et al.* Transparent, conductive carbon nanotube films. *Science* **305,** 1273–1276 (2004).
3. Snow, E. S., Perkins, F. K., Houser, E. J., Badescu, S. C. & Reinecke, T. L. Chemical detection with a single-walled carbon nanotube capacitor. *Science* **307,** 1942–1945 (2005).
4. Artukovic, E., Kaempgen, M., Hecht, D. S., Roth, S. & Gruner, G. Transparent and flexible carbon nanotube transistors. *Nano Lett.* **5,** 757–760 (2005).

5. Kang, S. J. *et al.* High-performance electronics using dense, perfectly aligned arrays of single-walled carbon nanotubes. *Nature Nanotech.* **2,** 230–236 (2007).
6. Fan, Z. *et al.* Wafer-scale assembly of highly ordered semiconductor nanowire arrays by contact printing. *Nano Lett.* **8,** 20–25 (2008).
7. Liang, X., Fu, Z. & Chou, S. Y. Graphene transistors fabricated via transfer-printing in device-active areas on large wafer. *Nano Lett.* **7,** 3840–3844 (2007).
8. Chen, J. H. *et al.* Printed graphene circuits. *Adv. Mater.* **19,** 3623–3627 (2007).
9. Meitl, M. A. *et al.* Transfer printing by kinetic control of adhesion to an elastomeric stamp. *Nature Mater.* **5,** 33–38 (2006).
10. Li, D., Muller, M. B., Gilje, S., Kaner, R. B. & Wallace, G. G. Processable aqueous dispersions of graphene nanosheets. *Nature Nanotech.* **3,** 101–105 (2008).
11. Novoselov, K. S. *et al.* Electric field effect in atomically thin carbon films. *Science* **306,** 666–669 (2004).
12. Geim, A. K. & Novoselov, K. S. The rise of graphene. *Nature Mater.* **6,** 183–191 (2007).
13. Schedin, F. *et al.* Detection of individual gas molecules adsorbed on graphene. *Nature Mater.* **6,** 652–655 (2007).
14. Han, M. Y., Ozyilmaz, B., Zhang, Y. B. & Kim, P. Energy band-gap engineering of graphene nanoribbons. *Phys. Rev. Lett.* **98**, 206805 (2007).
15. Barbolina, I.I. *et al.* Submicron sensors of local electric field with single-electron resolution at room temperature. *Appl. Phys. Lett.* **88,** 013901 (2006).
16. Tombros, N., Jozsa, C., Popinciuc, M., Jonkman, H. T. & van Wees, B. J. Electronic spin transport and spin precession in single graphene layers at room temperature. *Nature* **448,** 571–574 (2007).
17. Berger, C. *et al.* Ultrathin epitaxial graphite: 2D electron gas properties and a route toward graphene-based nanoelectronics. *J. Phys. Chem. B* **108,** 19912–19916 (2004).
18. Coraux, J., N'Diaye, A. T., Busse, C. & Michely, T. Structural coherency of graphene on Ir(111). *Nano Lett.* **8,** 565–570 (2008).
19. Stankovich, S. *et al.* Graphene-based composite materials. *Nature* **442,** 282–286 (2006).
20. Gomez-Navarro, C. *et al.* Electronic transport properties of individual chemically reduced graphene oxide sheets. *Nano Lett.* **7,** 3499–3503 (2007).
21. Gijie, S., Han, S., Wang, M., Wang, K. L. & Kaner, R. B. A chemical route to graphene for device applications. *Nano Lett.* **7,** 3394–3398 (2007).
22. Wang, X., Zhi, L. & Mullen, K. Transparent, conductive graphene electrodes for dye-sensitized solar cells. *Nano Lett.* **8,** 323–327 (2007).
23. Jung, I. *et al.* Simple approach for high-contrast optical imaging and characterization of graphene-based sheets. *Nano Lett.* **7,** 3569–3575 (2007).
24. Schniepp, H. C. *et al.* Functionalized single graphene sheets derived from splitting graphite oxide. *J. Phys. Chem. B* **110,** 8535–8539 (2006).
25. McAllister, M. J. *et al.* Single sheet functionalized graphene by oxidation and thermal expansion of graphite. *Chem. Mater.* **19,** 4396–4404 (2007).
26. Stankovich, S. *et al.* Stable aqueous dispersions of graphitic nanoplatelets via the reduction of exfoliated graphite oxide in the presence of poly(sodium 4-styrenesulfonate). *J. Mater. Chem.* **16,** 155–158 (2006).
27. Hirata, M., Gotou, T., Horiuchi, S., Fujiwara, M. & Ohba, M. Thin-film particles of graphite oxide 1: High-yield synthesis and flexibility of the particles. *Carbon* **42,** 2929–2937 (2004).
28. Hu, L., Hecht, D. S. & Gruner, G. Percolation in transparent and conducting carbon nanotube networks. *Nano Lett.* **4,** 2513–2517 (2004).
29. Unalan, H. E., Fanchini, G., Kanwal, A., Du Pasquier, A. & Chhowalla, M. Design criteria for transparent single-wall carbon nanotube thin-film transistors. *Nano Lett.* **6,** 677–682 (2006).
30. Stankovich, S. *et al.* Synthesis of graphene-based nanosheets via chemical reduction of exfoliated graphite oxide. *Carbon* **45,** 1558–1565 (2007).
31. Ferrari, A. C. *et al.* Raman spectrum of graphene and graphene layers. *Phys. Rev. Lett.* **97**, 187401 (2006).
32. Watcharotone, S. *et al.* Graphene–silica composite thin films as transparent conductors. *Nano Lett.* **7,** 1888–1892 (2007).
33. Uher, C. & Sander, L. M. Unusual temperature dependence of the resistivity of exfoliated graphites. *Phys. Rev. B* **27,** 1326–1332 (1983).

Supplementary information accompanies this paper at www.nature.com/naturenanotechnology.

Acknowledgements

The authors would like to acknowledge Yun-Yue Lin and S. Miller for fabricating organic photovoltaic devices. A detailed study on the photovoltaic devices will be reported elsewhere. We also acknowledge A. Kanwal for help with the low-temperature measurements, and thank O. Celik for help with XPS analysis and A. Mann for allowing us the use of the Raman instrument. This work was funded by the National Science Foundation CAREER Award (ECS 0543867).

Author contributions

G.E. and M.C. conceived and designed the experiments. G.E. carried out the exfoliation, dispersion and deposition processes in addition to conducting the opto-electronic and device measurements. G.F. performed the Raman analysis. M.C. wrote the paper with input from G.E. All the authors discussed the results and commented on the manuscript throughout the review process.

Author information

Reprints and permission information is available online at http://npg.nature.com/reprintsandpermissions/. Correspondence and requests for materials should be addressed to M.C.